ELSEVIER

Polymer 42 (2001) 4825–4835

polymer

www.elsevier.nl/locate/polymer

# The kinetics and mechanisms of the thermal degradation of poly(methyl methacrylate) studied by thermal analysis-Fourier transform infrared spectroscopy

B.J. Holland, J.N. Hay*

*Plastic Materials Laboratory, School of Metallurgy and Materials, The University of Birmingham, Edgbaston, Birmingham B15 2TT, UK*

Received 29 September 2000; received in revised form 30 November 2000; accepted 11 December 2000

**Abstract**

The kinetics and mechanisms of thermal degradation of poly(methyl methacrylate) (PMMA) have been studied to demonstrate the usefulness of thermal analysis-Fourier transform infrared spectroscopy (TA-FTIR) as a qualitative and quantitative kinetic tool to study the thermal degradation of polymers. From the dependence of the rate of thermal degradation of PMMA on molecular weight at low degradation temperatures, it was concluded that thermal degradation was initiated by a mixture of chain end and random chain scission initiation, followed by depropagation and first-order termination. Random scission is attributed to pre-oxidation of the polymer on storage at room temperature. At higher temperatures, a change in molecular weight dependence was observed, related to depropagation to the end of the polymer chain. The thermal degradation of PMMA also leads to the production of char, which was produced by the elimination of methoxycarbonyl side-chains. The amount of char produced increased with increasing concentration of end-groups and temperature.


*Keywords*: Poly(methyl methacrylate); Thermal analysis-Fourier transform infrared spectroscopy; Thermal degradation

## 1. Introduction

The thermal degradation of poly(methyl methacrylate) (PMMA) has been the subject of numerous publications [1–11]. PMMA is regarded as a polymer that depropagates to monomer as a result of thermal degradation up to 550°C [1–3]. Furthermore, the rate of thermal degradation has been found to depend upon the initial degree of polymerisation ($D$) of the polymer, the dependence of which has been used to identify the mechanisms of thermal degradation [4–7].

It has also been reported [8–11] that some degradation occurs by side-group elimination, leading to the production of unsaturated products. It has also been claimed that side-group elimination is a more dominant process than chain scission initiation, due to the possibility of efficient recombination of the caged radical chain ends [10,11].

In this study, the technique of thermal analysis-Fourier transform infrared spectroscopy (TA-FTIR) [12] has been applied to study the thermal degradation of PMMA, to demonstrate its use as a qualitative and quantitative method of studying thermal degradation. The main advantage of this method over pyrolysis-gas chromatography is that not only can the volatile products be analysed by infrared gas cell, but the polymer residue can be monitored during thermal degradation, and any significant changes in chemical composition determined.

## 2. Kinetic analysis of the thermal degradation of PMMA

It is generally accepted [1–7] that PMMA degrades predominantly by a depropagation process (as a reverse of the polymerisation process), the rate of which is first-order in weight loss, but this order is only accurately followed with time over an initial period. Using FTIR spectroscopy, the change in the number of monomer moles can be monitored directly by changes in the absorbance ($A$) of characteristic vibrational bands as shown below. From the Beer–Lambert Law,

$$A = \log \frac{I_0}{I} = \epsilon c l$$

where $I_0$ is the intensity of the incident infrared beam at a wavenumber at which a characteristic infrared absorption occurs, $I$ is the intensity of the infrared beam following

* Corresponding author. Tel.: +44-121-414-4544; fax: +44-121-414-5232.

*E-mail address:* j.n.hay@bham.ac.uk (J.N. Hay).

0032-3861/01/$ - see front matter 
PII: S0032-3861(00)00923-X

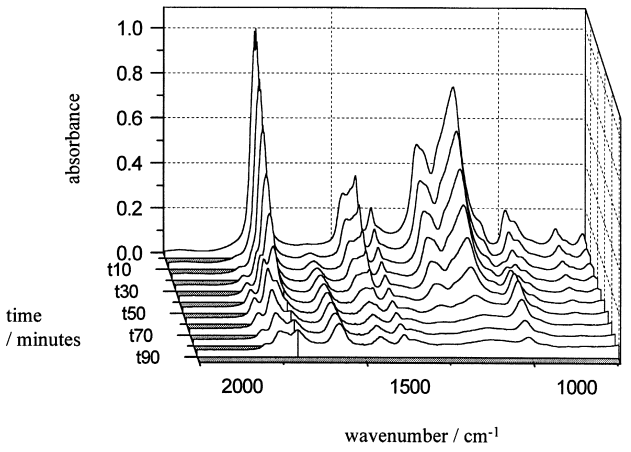


Fig. 1. TA-FTIR data for the thermo-oxidative degradation of PMMA at 340°C.

absorption, $\epsilon$ is the extinction coefficient for the characteristic infrared absorption, $c$ is concentration of material and $l$ is the thickness of sample through which the infrared beam passes. The concentration of molecules, $c = n/V$, where $n$ is the number of molecules in the system and $V$ the volume. Since $V = al$, where $a$ is the area of sample through which the infrared beam passes, then

$$A = \frac{\epsilon n l}{a l} = \left(\frac{\epsilon}{a}\right) n$$

Therefore, if $\epsilon/a$ remains constant for any particular experiment, then it is a direct measure of the number of moles of monomer in the sample.

If for the thermal degradation of PMMA, it is considered that the depropagation process can be initiated both by chain end and chain scission initiation, termination is a first-order process. Assuming a stationary state in the rate of change of radical concentration with time, the following relationship [7,13] can be derived for the first-order rate constant for the observed rate of degradation, $k_{(obs)}$,

$$k_{(obs)} = \left(\frac{k_i}{D} + 2k_i'\right)\frac{k_d}{k_t'} \quad (1)$$

where $k_i$ is the first-order rate constant for chain end initiation, $k_i'$ is the first-order rate constant for chain scission initiation, $k_d$ is the first-order rate constant for depropagation, $k_t'$ is the first-order rate constant for termination and $D$ is the degree of polymerisation. Hence, a plot of $k_{(obs)}$ versus $1/D$ for a range of molecular weights should be linear, with a slope and intercept related to the rate of chain end initiation and the rate of chain scission initiation, respectively.

If termination is by a bimolecular process, termination is a second-order process, and it can be shown that

$$k_{(obs)} = \left(\frac{k_i}{D} + 2k_i'\right)\frac{k_d u^{1/2}}{(2k_t\rho)^{1/2}} \quad (2)$$

where $k_t$ is the rate constant for second-order termination, $u$ is the molecular weight of the repeat unit and $\rho$ is the density of the polymer for a given temperature. Therefore, a plot of $k_{(obs)}$ versus $1/D^{1/2}$ should be linear.

Alternatively, if the kinetic chain length of the depropagation process is the same or greater than the length of the polymer chains, a radical can depropagate to the end of the polymer chain, termination will be volatilisation of the residual radical. In this case the rate of depropagation, and hence $k_{(obs)}$, is proportional to $D$.

## 3. Experimental

### 3.1. TA-FTIR

The apparatus for TA-FTIR spectroscopy was a combination of a Nicolet 760 IR-Magna infrared spectrometer, and a Linkam 600 microscope hot-stage unit placed in the beam of the spectrometer. The hot-stage unit, was fitted with barium fluoride windows suitable for infrared spectrometry in the range 4000–740 $cm^{-1}$, and was purged for 30 min with argon (300 $cm^3\ min^{-1}$) prior to each experiment. The same flow of argon was maintained throughout the experiment. The temperature of the hot-stage was calibrated with the melting points of KOH and NaOH. Isothermal temperatures between 340 and 420°C were chosen to study the thermal degradation of PMMA, using an initial heating rate of 90°C $min^{-1}$. This allowed the desired degradation temperature to be reached before significant degradation had occurred.

### 3.2. Procedure

Thin film samples of PMMA were placed on 16 mm diameter KBr disks from 5 $mm^3$ of a 4% (w:w) solution of chloroform and dried in a vacuum oven (80°C). Typically films of about 1 μm were made by this method, which was about the minimum film thickness which can be used whilst still achieving acceptable infrared absorbance, and is thin enough for sample size effects to be minimised [14]. The coated KBr disks were placed in the hot-stage unit, and degraded in the path of the infrared spectrometer beam.

For the purposes of kinetic analysis, infrared spectra were taken at regular intervals depending on the degradation temperature. For the temperature range 340–385°C, 10 min intervals were used, and each measurement comprised 256 scans. At 400°C, 64 scans were taken at 2 min intervals, and at 420°C 32 scans were taken at 1 min intervals. Absorbances were measured using Nicolet Omnic ESP software.

### 3.3. Effect of oxidation on PMMA

It was found that if the hot-stage unit was not sufficiently purged at the degradation temperatures used, oxidation of PMMA would occur. Oxidation manifested itself by the production of new absorption bands at 1820, 1775 and 1014 $cm^{-1}$, see Fig. 1. These bands may have been due to

Table 1
GPC analysis of PMMA

| Date polymerised | Date analysed | $M_p$ (GPC) | $M_w/M_n$ (GPC) | End-group |
|---|---|---|---|---|
| 11/2/99 | 27/9/99 | 12,700 | 1.03 | 2,2-diphenyl hexyl |
| 23/4/98 | 27/9/99 | 28,750 | 1.03 | 2,2-diphenyl hexyl |
| 22/4/97 | 27/9/99 | 69,000 | 1.03 | 2,2-diphenyl hexyl |
| 23/6/94 | 27/9/99 | 174,000 | 1.04 | 2,2-diphenyl hexyl |
| 28/11/97 | 27/9/99 | 518,900 | 1.03 | 2,2-diphenyl hexyl |
| 11/6/97 | 27/9/99 | 780,000 | 1.03 | 2,2-diphenyl hexyl |
| 21/10/00 | 27/9/99 | 1,520,000 | 1.08 | 2,2-diphenyl hexyl |
| Approx. 1985 | Approx. 1985 | 29,700 | 1.08 | cumyl |
| | 23/5/00 | 22,600 | 1.05 | |
| Approx. 1985 | Approx. 1985 | 460,000 | 1.14 | cumyl |
| | 23/5/00 | 344,500 | 1.24 | |

the production of acid peroxide, acid anhydride or unsaturated lactone groups [15], and are not consistent with the major volatile oxidation products of PMMA, which include methyl methacrylate, methyl pyruvate and 2-methyl-oxirane carbonic acid methyl ester [16]. The emergence of these bands was accompanied by a marked increase in the rate of degradation. No such bands were produced in the samples degraded under a sufficient flow of argon.

### 3.4. PMMA samples

Two sources of mono-disperse PMMA samples (with peak molecular weights, $M_p$, between 12,700 and 1,520,000) were supplied by Polymer Laboratories Ltd. The most recently obtained samples, approximately three years old, were terminated at one end by a hydrogen atom, and at the other end by a 2,2-diphenyl hexyl group. Older samples (approximately 15 years of age) of PMMA were also studied, to see if there was any effect of storage on thermal degradation. These were terminated by a hydrogen atom at one end, and a cumyl group at the other. A full list of PMMA samples used is shown in Table 1.

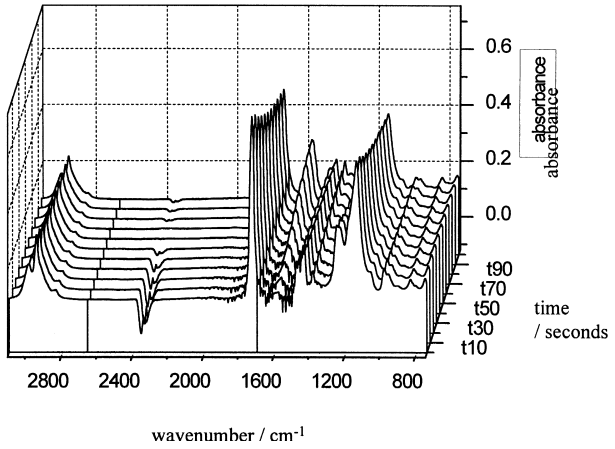


Fig. 2. TA-FTIR data for the thermal degradation of PMMA ($M_p$ = 12,700) at 370°C.

### 3.5. Thermogravimetry

For comparative purposes, thermogravimetry (TG) was carried out on selected samples at isothermal temperatures between 370 and 420°C. A Stanton Redcroft STA 1000 thermogravimetric balance with a type R (platinum–rhodium) thermocouple placed close to a platinum sample crucible was used. A sample size of 30 mg and a 40 $cm^3\,min^{-1}$ flow of argon gas was chosen. Sample size and gas flow had no effect on the measured isothermal weight loss versus time plots.

## 4. Results and discussion

### 4.1. Changes in PMMA residue during thermal degradation

Typical changes in the infrared spectra of PMMA with time at 370°C are shown in Figs. 2 and 3. First-order rate

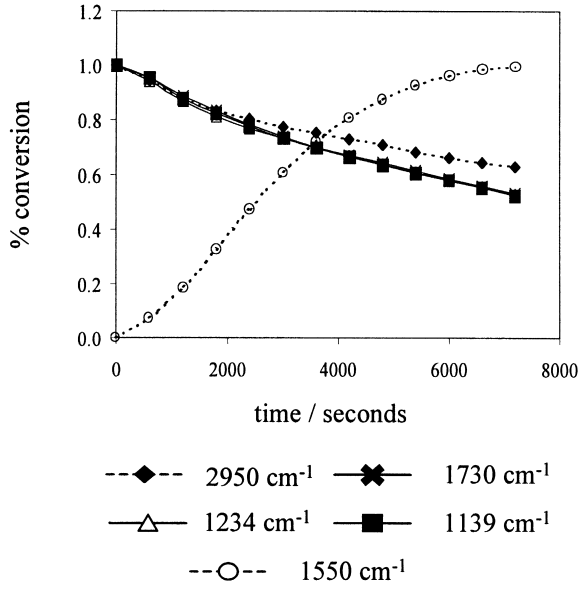


Fig. 3. Change in absorbance of selected infrared bands of PMMA ($M_p$ = 12,700) at 370°C.

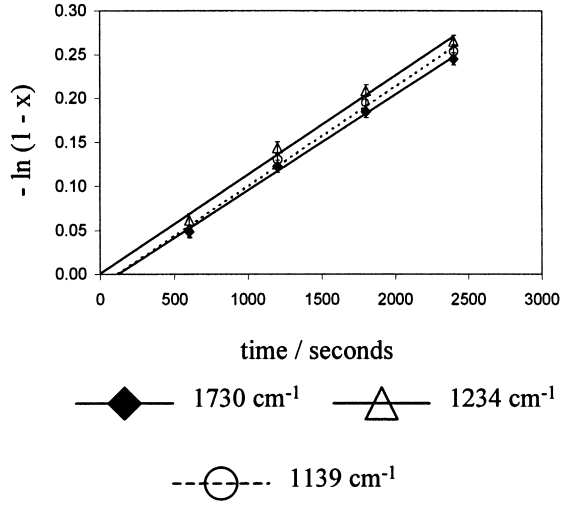


Fig. 4. First-order rate plot for loss of absorbance of selected infrared bands of PMMA ($M_p = 12,700$) at 370°C.

plots for the change in absorbance of the vibrational bands at 1730, 1234 and 1139 $cm^{-1}$ showed good linearity (Fig. 4) up to 20% conversion. It was noted, however, that a new peak developed with time at 1550 $cm^{-1}$. At high conversion, the $C–H_{(str)}$ band at 2950 $cm^{-1}$ did not disappear completely during thermal degradation. In addition, the PMMA film turned brown during thermal degradation, and the samples of PMMA used, produced char.

Fig. 5 shows the infrared spectrum of the final residue produced on degradation at 420°C. Band assignations are shown in Table 2. The unsaturated band of the PMMA char appeared at a significantly lower wavenumber (1550 $cm^{-1}$) than expected and was highly intense, indicative of the presence of a conjugated system. The wavenumber of this peak was too low to be associated with the formation of unconjugated unsaturated groups (usually 1680–1620 $cm^{-1}$). In addition, the infrared spectrum of the PMMA char indicated the presence of methyl side-groups (1380 $cm^{-1}$) and that the structure around the double bonds is likely to be R1R2C=CHR3 (840 $cm^{-1}$) [17]. A similar

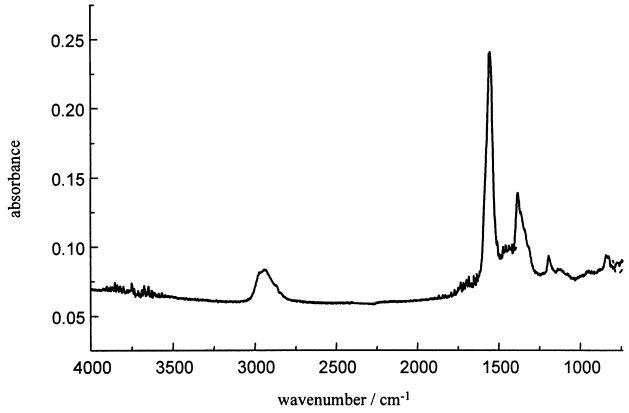


Fig. 5. Infrared spectra of PMMA char.

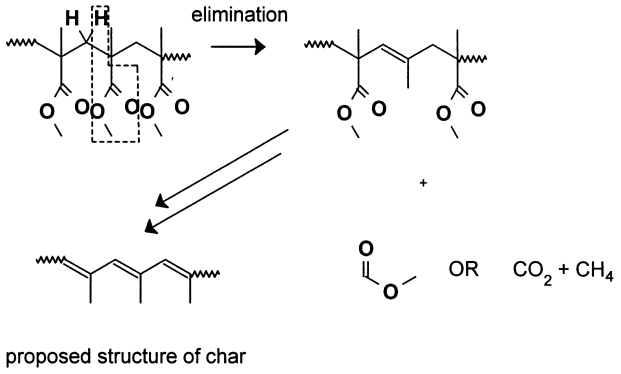


Fig. 6. Proposed mechanism of side-group elimination in PMMA.

structure to poly(isoprene) with a conjugated system is suggested for the char product.

It is clear that the char was produced by side-group elimination (Fig. 6) by scission of the C–C bond of the methoxycarbonyl side-group [8–11]. A relative measurement of the amount of char (which is related to the amount of conjugation) formed during degradation, can be made by dividing the absorbance of the conjugated C=C band (*c*), at a given time with that of the initial height of the carbonyl band (*m*). A plot of *c*/*m* versus degradation time for samples of different molecular weights at 370°C is shown in Fig. 7. The final *c*/*m* values for the molecular weight range, at 370 and 420°C were calculated, and when *c*/*m* was plotted against 1/*D* in Fig. 8, a straight-line relationship was observed with a positive intercept. The amount of conjugation, hence char, produced is clearly dependent on the number of polymer chain ends. At 420°C, more char was observed than at 370°C, and it was found that the slope of $k_{(obs)}$ versus 1/*D* was similar, but the intercept had increased, by approximately

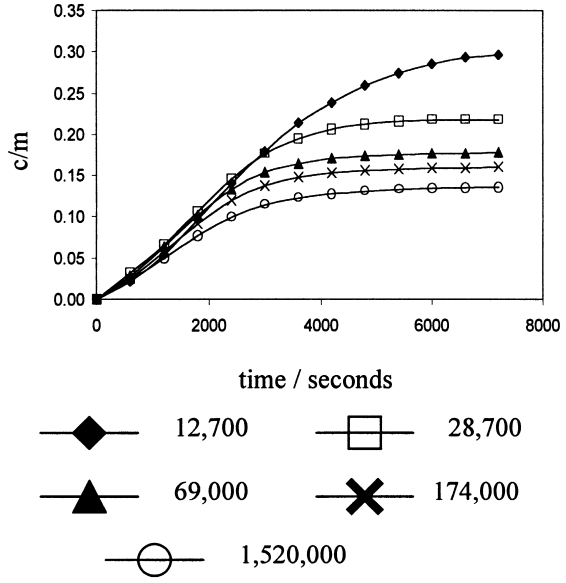


Fig. 7. Build-up of conjugation band at 1550 $cm^{-1}$ with time.

Table 2
Band assignments for the infrared spectrum of PMMA char

| | Band frequency ($cm^{-1}$) | Intensity | Group |
|---|---|---|---|
| PMMA char | 2950–2850 | Medium | Alkane $C–H_{(str)}$ |
| | 1550 | Strong | $C=C_{(str)}$ conjugated |
| | 1385 | Medium | $C–(CH_3)_{2\ (def)}$ |
| | 1375 | Shoulder | $C–(CH_3)_{(def)}$ |
| | 1350 | Shoulder | $–CH–_{(def)}$ |
| | 1170 | Weak | $C–(CH_3)_2$ skeletal vibration |
| | 840 | Weak | $R_1R_2C=CHR_3$ |

two. This shows that there is increasing involvement of side-group elimination along the polymer chain with temperature. It should be noted that even at moderate conversions, the actual degree of polymerisation is likely to be different from the initial degree of polymerisation. In which case, the change in the amount of char produced with $1/D$ should not be regarded as being due to the initial number of polymer chain ends, but the number of chain ends present at any given time.

The evolution of the conjugated unsaturation band with fractional degradation of polymer at 370°C is shown in Fig. 9. For the first 20% conversion, similar amounts of conjugation are produced at all values of $1/D$. However, above 20% conversion, the samples of lower initial $D$ produced more conjugation. This may have been due to a greater number of unsaturated end-groups, as C=C from previous scission or from activation by the 2,2-diphenyl hexyl terminal group, joining with unsaturated groups from side-chain elimination, following depropagation (see Fig. 10).

From TG studies (see Table 3) at 370°C it was observed that for PMMA samples of different molecular weight ($M_p$) of 12,700 and 1,520,000 different amounts of char were produced, 5.8 and 3.0 wt%, respectively. The ratio of these two values ($1.93 \pm 0.19$) was consistent with the $c/m$ values determined by TA-FTIR ($2.17 \pm 0.26$). At 420°C, 5.0% char was recovered from PMMA with an $M_p$ of 1,520,000, giving a ratio of $1.67 \pm 0.17$ with that at 370°C, and $c/m$ values from TA-FTIR give a ratio of $2.03 \pm 0.29$. This indicates that although TA-FTIR cannot be used to calculate the absolute amount of char, the relative yields of char determined by TA-FTIR were consistent with those found by TG.

Using the structure identified for the char from its infrared spectrum, it was possible to calculate the amount of PMMA converted to char during the TG experiments. The relative molecular mass of a repeat unit of the char is 40 g $mol^{-1}$, whereas that of PMMA is 100 g $mol^{-1}$. At 370°C, 14.5 and 7.5% of the PMMA is turned to char for $M_p$ of 12,700 and 1,520,000, respectively, and at 420°C, 12.5% of PMMA of $M_p$ 1,520,000 converts to char. Such proportions of PMMA converting to char must alter the overall thermal degradation kinetics and the kinetic order with increasing conversion.

A significant amount of char formation in degradation could result in an incorrect estimate of the rate of degradation. In a situation where the rate of degradation was measured through the quantity of volatiles produced from an initial short burst, followed by a complete burn off of volatiles, the burn off would underestimate the limiting yield of material being degraded. This would lead to an

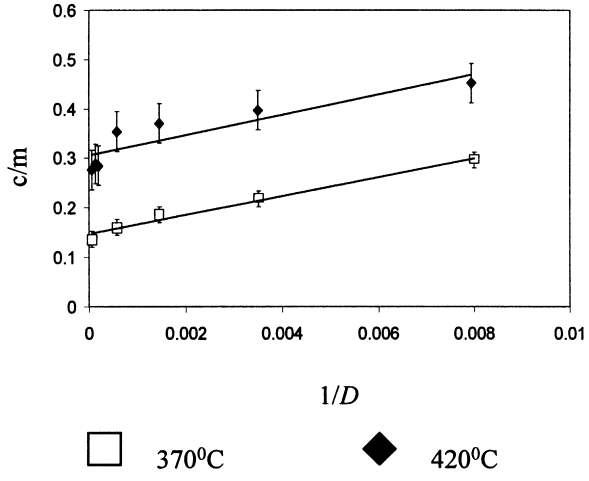


Fig. 8. Plot of final $c/m$ value versus $1/D$, for thermal degradation of PMMA at 370 and 420°C.

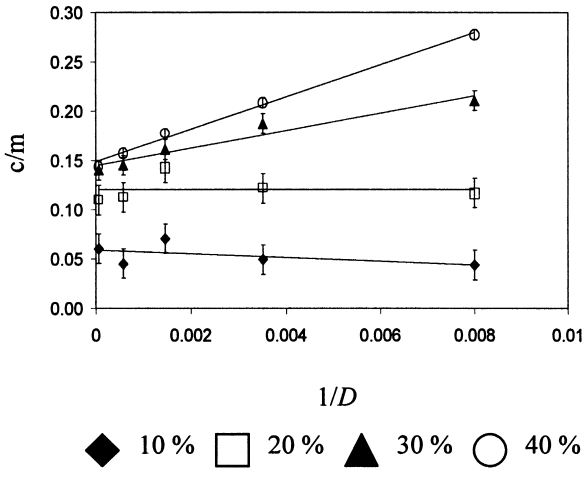


Fig. 9. Plot of $c/m$ at a certain fractional conversion versus $1/D$, for thermal degradation at 370°C.

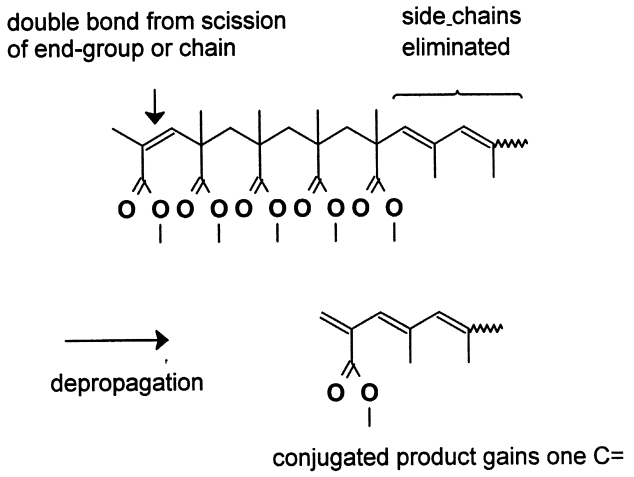


Fig. 10. Proposed mechanism for end-group contribution to the infrared band at 1550 $cm^{-1}$.

overestimate of the fractional conversion, and the observed rate constant.

In TA-FTIR spectroscopic studies, kinetic measurement based on the change in absorbance of vibrational bands related to the methoxycarbonyl side-group (1730, 1234 & 1139 $cm^{-1}$), would lead to an overestimate in loss of material attributed to conversion to monomer, because side-groups are also lost by elimination. However, the total amount of material, which is measured at the beginning of the experiment, would not be affected. TA-FTIR spectroscopy has the advantage that in the early stages of degradation, the rate of char formation does not vary much with molecular weight, whereas in the burn-off situation where maximum conversion has to be achieved, the amount of char varies greatly with temperature and molecular weight. Hence, the error in measured $k_{(obs)}$ due to char formation for TA-FTIR spectroscopy is likely to be smaller in size and more consistent.

### *4.2. A comparison of rate constants obtained by TA-FTIR spectroscopy and TG*

Initial first-order rate constants for the thermal degradation of PMMA measured by TG and TA-FTIR are shown in Table 4. The values are in good agreement, and differences are likely to be due to the different sample sizes, sample thickness and architecture of the furnaces and thermocouples used.

### *4.3. The kinetics of thermal degradation of PMMA by TA-FTIR*

Assuming, as discussed above, that the effect of char formation on the overall rate of loss of infrared bands related to the methoxycarbonyl side-group is small at low conversion and consistent, the loss of the 1139 $cm^{-1}$ infrared band ($O-CH_{3(str)}$) with time was used to measure the extent of thermal degradation. Six isothermal temperatures were chosen in the range 340–420°C and up to seven materials of different molecular weights were degraded at each temperature. The results for the different temperatures will be discussed in the following sections and are summarised in Table 5.

#### *4.3.1. Low temperature range (340–361°C)*

At these temperatures the rates of thermal degradation were low (typically of the order $10^{-5}$ $s^{-1}$). First-order rate plots for the loss of absorbance with time, were typically linear for the first 20% conversion, over which $k_{(obs)}$ was calculated. Plots of $k_{(obs)}$ versus $1/D$ for each temperature were linear, with an intercept above zero (see Fig. 11), consistent with Eq. (1). This indicated that initiation was a mixture of both chain end and random chain scission initiation, and that termination was by a first-order process. Previously, it has been shown that at low degradation temperatures, degradation was initiated at chain ends only

Table 3
Measurement of char yield by TG and TA-FTIR

| Degradation temperature (°C) | Molecular weight | Percentage char by TG (%) | TA-FTIR *c*/*m* value |
|---|---|---|---|
| 370 | 12,700 | 5.8 ± 0.6 | 0.296 ± 0.017 |
| | 1,520,000 | 3.0 ± 0.3 | 0.136 ± 0.016 |
| 420 | 1,520,000 | 5.0 ± 0.5 | 0.276 ± 0.040 |

Table 4
Comparison of first-order rate constants for the thermal degradation of PMMA measured by TG and TA-FTIR

| Degradation temperature (°C) | Molecular weight | Estimation of $k_{(obs)}$ by TG ($s^{-1}$) | Estimation of $k_{(obs)}$ by TA-FTIR ($s^{-1}$) |
|---|---|---|---|
| 370 | 12,700 | $(1.29 \pm 0.14) \times 10^{-4}$ | $(1.130 \pm 0.002) \times 10^{-4}$ |
| | 1,520,000 | $(1.03 \pm 0.12) \times 10^{-5}$ | $(8.36 \pm 0.02) \times 10^{-5}$ |
| 420 | 1,520,000 | $(1.02 \pm 0.08) \times 10^{-2}$ | $(8.73 \pm 0.05) \times 10^{-3}$ |

Table 5
Mechanistic implications of the dependence of $k_{(obs)}$ on $D$

| Degradation temperature (°C) | Dependence of $k_{(obs)}$ versus $D$ | Proposed mechanism |
|---|---|---|
| 340 | $k_{(obs)}$ versus $1/D$ linear with intercept | Chain end and chain scission initiation, first-order termination |
| 361 | $k_{(obs)}$ versus $1/D$ linear with greater slope and intercept than 340°C | Chain end and chain scission initiation, first-order termination |
| 370 | $k_{(obs)}$ versus $1/D$ appears slightly curved, with lower slope than 360°C | Chain end and chain scission initiation, first-order termination combined with very small amount of depropagation to chain end |
| 385 | $k_{(obs)}$ versus $1/D$ almost horizontal | Chain end and chain scission initiation, first-order termination combined with depropagation to chain end makes plot appear almost horizontal |
| 400 | $k_{(obs)}$ versus $D$ linear at low $D$ with intercept | Chain end and chain scission initiation, depropagation to chain end predominates at low $D$, at higher $D$ first-order termination may occur |
| 420 | $k_{(obs)}$ versus $D$ linear at low $D$ with intercept | Chain end and chain scission initiation, depropagation to chain end predominates at low $D$, at higher $D$ first-order termination may occur |

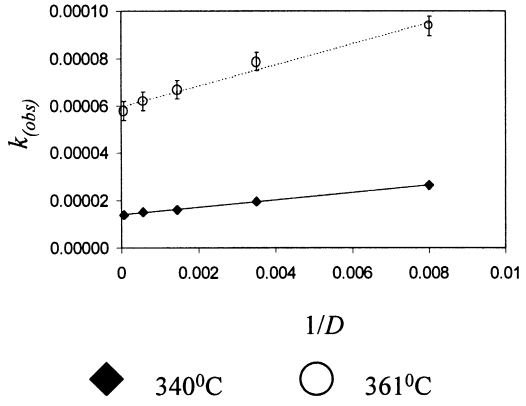


Fig. 11. Plot of $k_{(obs)}$ versus $1/D$ for PMMA at 340 and 361°C.

[6,7] ($k_{(obs)}$ versus $1/D$ passed through the origin). However, in this study this is not the case.

Although the $k_{(obs)}$ versus $1/D$ relationship only held for the lower temperature situations, an attempt was made to quantify the activation energy of chain end initiation and chain scission initiation processes by measuring the slope and intercept for each temperature, calculating the activation energy from an Arrhenius relationship, and the relationships from Eq. (1),

$$\text{slope} = \frac{k_i k_d}{k_t'}$$

$$\text{intercept} = \frac{2k_i' k_d}{k_t'}.$$

The activation energy for chain end initiated and chain scission initiated degradation processes was found to be $150 \pm 25$ and $210 \pm 40$ kJ mol$^{-1}$, respectively. This indicates that it is marginally easier to break an end-group than a bond in the polymer backbone, probably because the phenyl groups of the 2,2-diphenyl hexyl group activate

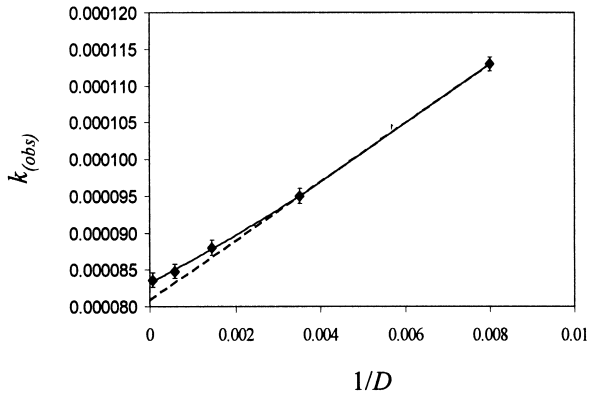


Fig. 12. Plot of $k_{(obs)}$ versus $1/D$ for PMMA at 370°C.

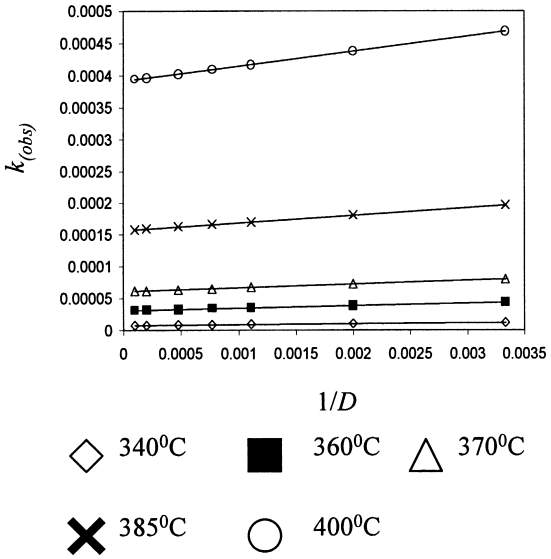


Fig. 13. Theoretical kinetic data, calculated from low temperature kinetic data, to show the effect of chain end and chain scission initiation on the dependence of $k_{(obs)}$ with $1/D$.

the C–C bond linked to the polymer chain. The bond enthalpy for a C–C bond is quoted [18] as 348 kJ mol$^{-1}$, which is somewhat higher than predicted for the chain scission and chain end initiated processes, the values of which may have been affected by the $k_d$ and $k'_t$ terms associated with them.

These differences may reflect differences in the terminal units, i.e. lauryl mercaptyl units (used previously) and 2,2-diphenyl hexyl units (used in this study), and may also account for the difference in observed rate constants between the two polymer systems studied. The bond enthalpies associated with C–C bonds and C–S bonds are 348 and 259 kJ mol$^{-1}$, respectively [18]. Therefore the C–S bond that links the mercaptyl end-group to the PMMA chain can be more readily broken than the C–C bond that links the 2,2-diphenyl hexyl group to the PMMA chain. Hence chain end initiation is more likely in the case where lauryl mercaptyl end-groups were used.

#### 4.3.2. Intermediate temperature (370°C)

At first glance, the plot of $k_{(obs)}$ versus $1/D$ at 370°C appeared to be linear (Fig. 12). However, it should be noted that the slope is less than that at 361°C. It is suggested that at low values of $1/D$, there is some curvature in the dependence. It has previously been claimed [6,7] that the slope of $k_{(obs)}$ versus $1/D$ reduces at higher temperature due to the predominance of random scission. However, this would require that the rate constant for chain end initiation would have to reduce with increasing temperature, which is most unlikely. The kinetic parameters collected at 340 and 361°C were used to determine the rate constants for $k_{(obs)}$ versus $1/D$ for a range of temperatures (Fig. 13), and it is obvious that as the temperature increased, so did the value of the slope and intercept.

Therefore, there must be an additional process, which is causing the curvature in Fig. 12, which indicates a bonus in rate constant at high values of $D$. The origin of this bonus will be discussed in the next section.

#### 4.3.3. High temperatures (385–420°C)

The dependence of $k_{(obs)}$ with $1/D$ at higher temperatures (385–420°C) can be seen in Fig. 14. It is clear that there is an additional process occurring at higher temperature, which has a greater effect on samples of high $D$. If this is due to the kinetic chain length of depropagation being greater than the length of the polymer chain, the depropagation process will terminate by volatilisation of a small chain end radical, and the rate of termination will depend upon the number of chain ends ($1/D$). That is,

$$\text{rate of termination} = k_v[R^{\cdot}]\left[\frac{1}{D}\right]$$

where $k_v$ is the rate constant for termination by volatilisation of a small radical. In deriving Eq. (1) replacing the first-order termination step with that for depropagation to a chain end, changes Eq. (1) to

$$k_{(obs)} = (k_i + 2k_i D)\frac{k_d}{k_v} \tag{3}$$

and, $k_{(obs)}$ now has a dependence on $D$. Plots of $k_{(obs)}$ versus $D$ at 385, 400 and 420°C are shown in Fig. 15(a)–(c), respectively. At low values of $D$ (up to 689 units), the plot of $k_{(obs)}$ versus $D$ is linear, but at higher values of $D$, deviates from linearity, due to longer chains terminating by radical disproportionation or addition. For these chains, the kinetic chain length of depropagation is less that the total length of the polymer chain, and the dependence of $k_{(obs)}$ on $D$ expressed in Eq. (1) should be considered as part of the overall dependence.

From Eq. (3), it is clear that the linear portion of a plot of $k_{(obs)}$ versus $D$ would have a slope of $2k'_i k_d/k_v$, which is the rate constant for the process of chain scission initiation, followed by depropagation to a chain end. Furthermore, the intercept would be $k_i k_d/k_v$, which is the rate constant for the process of chain end initiation, followed by depropagation to a chain end. The activation energy for the process of depropagation to a chain end was calculated as $190 \pm 10$ and $450 \pm 20$ kJ mol$^{-1}$, for chain end and chain scission initiation, respectively. The activation energy for chain end initiation is similar to that found at low temperature ($150 \pm 25$ kJ mol$^{-1}$). However, the activation energy calculated for chain scission initiation is high. In addition, the rate constants estimated in this way were very low ($2.9 \times 10^{-6}$–$2.4 \times 10^{-8}$ s$^{-1}$) compared to the low temperature ($k_{(obs)}$ versus $1/D$) results ($1.4 \times 10^{-5}$ to $6 \times 10^{-5}$ s$^{-1}$). It is likely that char formation, or changes in $D$ during thermal degradation would have affected the observed rate of thermal degradation. Furthermore, dominance of the chain end initiation process at high temperature, followed by depropagation to the end, will limit the opportunity for chain scission initiation to occur.

The observed rate constant for thermal degradation at 385°C appeared to have little dependence on $1/D$ (compared to results at 400 and 420°C). Previously, this has been associated with a situation where chain scission predominates, but as Fig. 14 shows, the slope of a plot of $k_{(obs)}$ versus $1/D$ should become steeper with increasing temperature (because $k_i$ increases with temperature). Hence, it is considered that the absence of a significantly larger slope at 385°C is due to the depropagation to chain end mechanism increasing $k_{(obs)}$ more, at lower values of $1/D$.

### 4.4. Effect of sample age on the kinetics of thermal degradation of PMMA

Standard mono-disperse PMMA samples ($M_p = 29,700$ and 460,000), used as molecular weight standards for GPC for about 15 years, were also degraded at 370°C by TA-FTIR spectroscopy, for the purpose of comparison. It was noticed that the infrared spectrum of the lower molecular weight sample contained an additional weak band at about 1600 cm$^{-1}$, indicative of the presence of some double

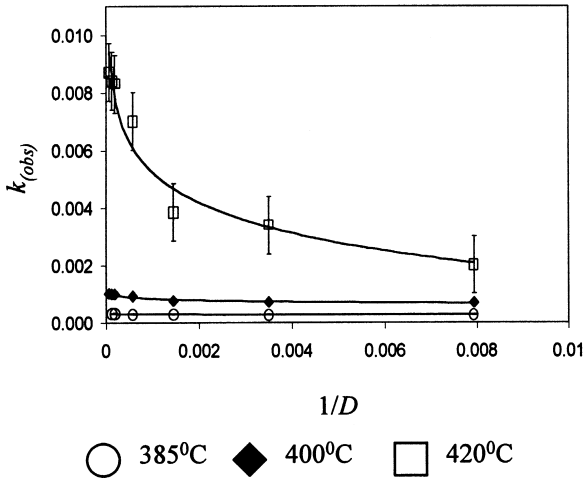


Fig. 14. Plot of $k_{(obs)}$ versus $1/D$ for PMMA at 385, 400 and 420°C.

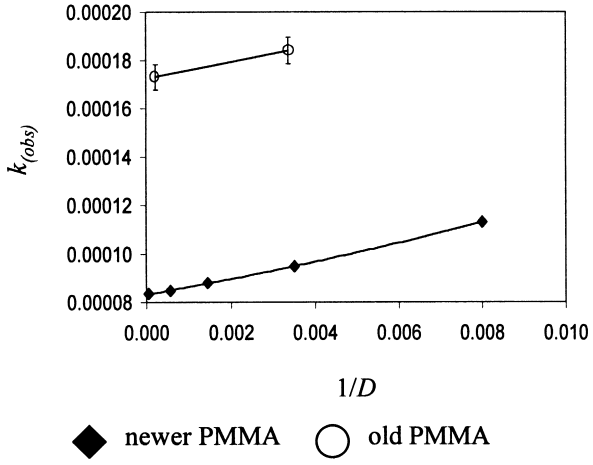


Fig. 16. Plot of $k_{(obs)}$ versus $1/D$ for old and new PMMA degraded at 370°C.

bonds, perhaps due to oxidation on storage. The molecular weight and polydispersity of the samples, measured by GPC, did not change appreciably on storage (see Table 1). The rate constants for the thermal degradation of these samples were greater than those of the newer samples, see Fig. 16, although the slope of the plot of $k_{(obs)}$ versus $1/D$ did not change, which indicated that end-groups of both materials were equally effective in causing chain end initiation. The amounts of char produced by the old materials were found to be greater (see Fig. 17). For $M_p$ values of 29,700 and 460,000, the $c/m$ values calculated were $0.325 \pm 0.026$ and $0.144 \pm 0.013$, respectively. The amount of char formed by the $M_p = 29,700$ sample was even greater than would be expected at an $M_p$ of 12,700.

The intercepts of the plots in Fig. 16 were taken and plotted against approximate sample age (Fig. 18(a)) and the square root of sample age (Fig. 18(b)). It is evident,

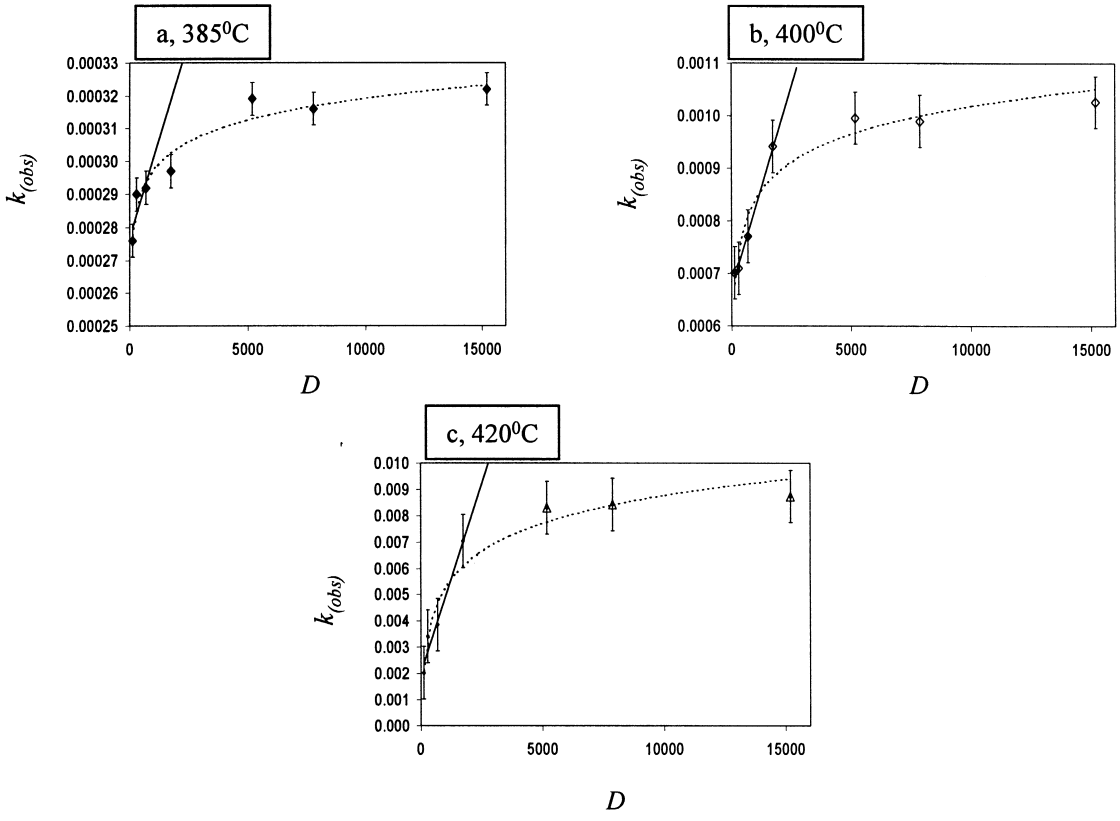


Fig. 15. Plot of $k_{(obs)}$ versus $D$ for PMMA at (a) 385°C, (b) 400°C and (c) 420°C.

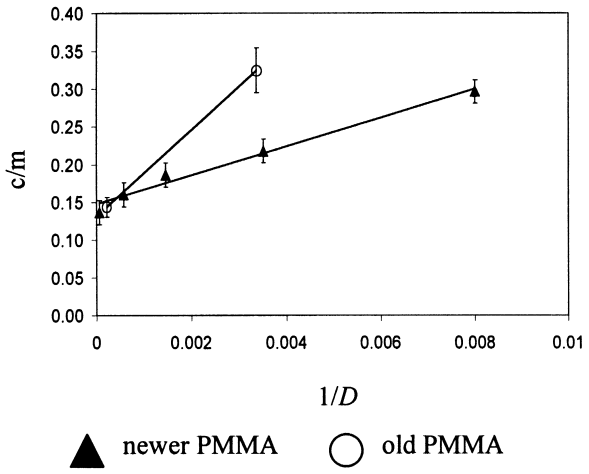


Fig. 17. Plot of $c/m$ versus $1/D$ for old and new PMMA degraded at 370°C.

within the experimental error, that the intercept of $k_{(obs)}$ versus $1/D$ increases with sample age, indicating increasing contribution of random scission initiation. If the contribution of random scission was proportional to the sample age, see Fig. 18(a), the intercept in this plot would indicate that some random scission occurs during the thermal degradation of newly polymerised samples. If the contribution of random scission was proportional to the square root of the sample age, see Fig. 18(b), the closeness of the straight line to the origin indicates that random scission would not occur in a newly polymerised sample. This dependence would be consistent with a diffusion controlled oxidation process, such as peroxidation during storage in air at room temperature, or the product of degradation of the peroxide, leading to random scission through degradation of the oxidation product during thermal degradation. However, it was considered that the oxidation products responsible for random scission were of too low a concentration to be detected by infrared spectroscopy. If oxidation during storage lead to random scission, a newly polymerised sample of PMMA would not degrade by a random scission initiation process, and only chain end initiation would occur. This might explain the variability in degradation rate constants of PMMA reported elsewhere [4–6].

## 5. Conclusions

The technique of TA-FTIR spectroscopy has been used to study the kinetics of thermal degradation of PMMA. In addition, it can provide a considerable amount of information about chemical changes occurring in the polymer residue, which is an advantage over many other techniques of studying thermal degradation.

Kinetic data extracted by TA-FTIR showed that at lower degradation temperatures (340–361°C), the mechanism of thermal degradation was initiated by a mixture of chain end and chain scission processes, followed by depropagation, and first-order termination. At higher temperatures, initiation was by a mixture of chain end and chain scission processes, followed by depropagation to the end of the polymer chain. However, at higher molecular weights, where the length of the polymer chain exceeded the average kinetic chain length, some first-order termination could occur. It also may be the case that a large kinetic chain length of depropagation may reduce the opportunities for chain scission to occur.

PMMA produces char. The process appears to be elimination of the methoxycarbonyl side-group, producing an unsaturated conjugated system. The amount of char yielded varies with molecular weight and temperature, and in some cases, it is estimated that 15% (or possibly even more) of the PMMA structure can degrade in this way. Given the amount of conjugated char produced, it was considered that side-chain elimination was unlikely to be an initiation route for depropagation.

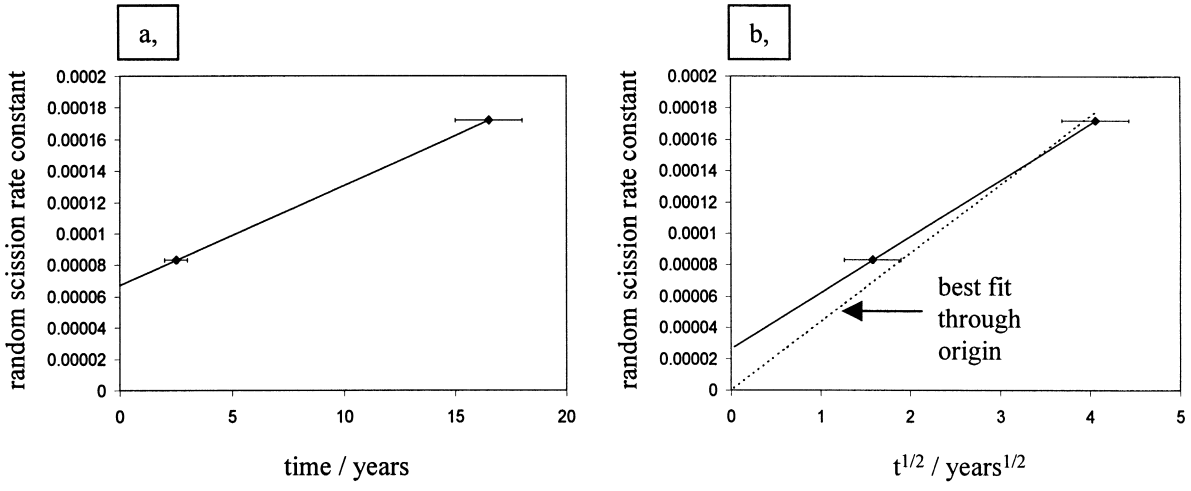


Fig. 18. Plot of $k_{(obs)}$ for random scission only versus (a) sample age and (b) $(\text{sample age})^{1/2}$.

Random scission initiation appears to be related to the age of the PMMA sample, and hence probably oxidation of the sample in storage, which does not cause scission of the PMMA at room temperature. Chain end initiation is due to the activating effect of the 2,2-diphenyl hexyl or cumyl groups used to terminate the polymer. Furthermore, the observation that all random scission occurs by peroxide degradation, leads to the conclusion that side-group initiation [10,11] of chain depropagation, which would have a similar dependence on *D* to random scission, is unlikely to occur.

## Acknowledgements

We are grateful to A. Bouffin of the University of Aston for GPC analysis of PMMA samples.

## References

[1] Grassie N, Melville HW. Proc R Soc 1949;199:1.
[2] Barlow A, Lehrle RS, Robb JC. Polymer 1961;2:27.
[3] Lehmann FA, Brauer GM. Anal Chem 1961;33:673.
[4] Barlow A, Lehrle RS, Robb JC, Sunderland D. Polymer 1967;8:537.
[5] Bagby G, Lehrle RS, Robb JC. Makromol Chem 1968;119:122.
[6] Bagby G, Lehrle RS, Robb JC. Polymer 1969;10:683.
[7] Lehrle R, Atkinson D, Cook S, Gardner P, Groves S, Hancox R, Lamb G. Polym Degrad Stab 1993;42:281.
[8] Manring LE. Macromolecules 1988;21:528.
[9] Manring LE. Macromolecules 1989;22:2673.
[10] Manring LE, Sogah DY, Cohen GM. Macromolecules 1989;24: 4652.
[11] Manring LE. Macromolecules 1991;24:3304.
[12] Holland BJ, Hay JN. Polym Int 2000;49:943.
[13] Lehrle RS, Peakman RE, Robb JC. Eur Polym J 1982;18:517.
[14] Bate DM, Lehrle RS, Pattenden CS, Place EJ. Polym Degrad Stab 1998;62:73.
[15] Williams DH, Fleming I. Spectroscopic methods in organic chemistry. 4th ed. London: McGraw Hill, 1989 (p. 47).
[16] Song J, Fischer Ch-H, Schnabel W. Polym Degrad Stab 1992;36:261.
[17] Bellamy LJ. The infrared spectra of complex molecules. 3rd ed. London: Chapman & Hall, 1975 (p. 38).
[18] Atkins PW. Physical chemistry. 4th ed. Oxford: Oxford University Press, 1990 (p. 938).